Journal of
Renewable Energy Research and Applications (RERA)

Published online

Comparison of BEM and FVM Approaches for Analysis of an Offshore Wind Turbine Installed on TLP in Caspian Sea

S. E. Kashfi[1], A. Ebrahimi[2*] and S. Kazemi[1]

1. Islamic Azad University, Science and Research Branch, Tehran, Iran.
2. Chabahar Maritime University, Chabahar, Iran.

Received Date 10 December 2022; Revised Date 04 January 2023; Accepted Date 09 January 2023
**Corresponding author: ab_ebrahimi@cmu.ac.ir (A. Ebrahimi)*

Abstract
Compliant offshore tension leg platforms (TLPs) are adaptive platforms with a vertical mooring system. These types of platforms are usually used in deep water. Adding sufficient initial tension to the mooring will reduce the vertical movements of the structure. This platform includes tendons, body, and deck, in which most hydrodynamic forces are applied to the body. In this work, an investigation is done on a TLP with a wind turbine by numerical analysis. The boundary element and the finite volume method are carried out in this work in the Caspian sea. Then the platform is analyzed at a depth of 150 m, under the influence of wind, current, and irregular waves with one and 100-year return period, and at a zero-degree wave angle. The results of the two numerical approaches are very close and almost identical. The tension leg platform is stable in the different irregular waves. Also the response amplitude operator calculated using two numerical methods agrees satisfactorily.

Keywords: *TLP, BEM, FVM, Wind Turbine, Irregular Wave, Response Amplitude Operators.*

1. Introduction

Compliant offshore platforms are constructed from steel or concrete and have large dimensions. These platforms are mainly used for oil and gas exploration and extraction. However, today, many countries are interested in using alternative energy sources. Wind energy is one of the high-efficiency strategies for generating energy among other clean sources such as ocean waves, thermal, and solar panels. It is emphasized that the combination of some sources as wind and ocean has also been considerably investigated recently by the researchers [1]. The potential of wind energy in deep locations of the ocean is high. For this reason, one of the usable platforms for supporting wind turbines is TLP.

For this reason, the platform that can be used to install wind turbines is TLP. TLP is one of the platforms that has worked successfully in deep water for oil extraction drilling. As a result, research is required to evaluate the performance of these platforms with a wind turbine under different waves. Both numerical analyses should consider all connections between the compliant offshore platform and the seabed. Mooring systems, pre-tension mooring lines, non-tension mooring lines, belt connections, connections for the launch of vessels, and oil transfer pipes from the structure to the seabed are all included in these two methods. The mooring system is a type of these connection used for TLP, semisubmersible, spar, and SPM. The schematic of TLP used in this research work, 6 degrees of freedom, and numbering of mooring lines are shown in figure 1.

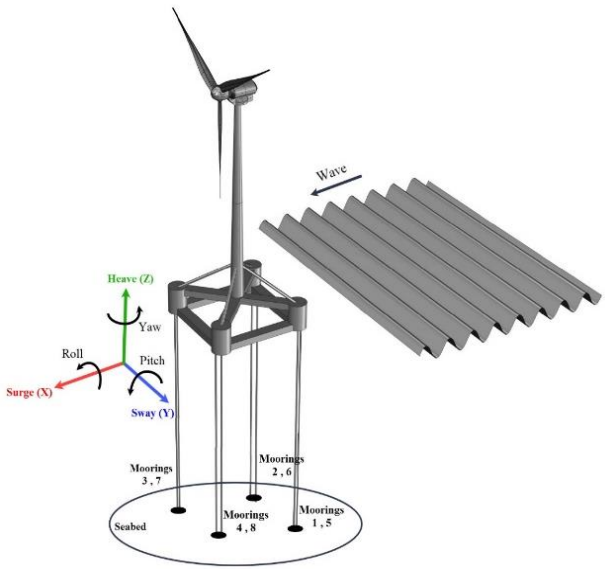

Figure 1. 6 DOF motions of TLP and mooring lines.

Some research works have been done on the hydrodynamic analysis of tension leg platforms. Han *et al*. [2] investigated a TLP with a wind turbine. They examined the TLP motions in all degrees of freedom under different environmental conditions at 150-170 m depth. Oguz *et al*. [3] numerically and experimentally studied the TLP motions at a depth of 70 in irregular waves. The forces applied on the platform deck and the mooring system of a TLP were analyzed by Abdussamie *et al*. [4]. This time-domain study was conducted experimentally with a scale of 1:125. Abrishamchi *et al*. [5] studied the hydrodynamic loads on the TPL leg and the vortex behind the legs. Kim *et al*. [6] investigated the dynamic response of TLP impacted by regular waves. Bachynski *et al*. [7], in addition to wave loads on TLP, considered the wind load on the platform deck and its effect on the tension of moorings. Senjanovic *et al*. [8] proposed a new stiffness matrix to analyze tension leg platforms. Yu *et al*. [9] investigated the hydrodynamic behavior of a TLP at different angles under a 100-year regular wave load. Gu *et al*. [10] used a stiffness matrix to study the dynamic behavior of a TLP platform under the effect of the wave, wind, and current forces. The dynamic response of a new TLP under regular and irregular waves was investigated numerically and experimentally by Ren *et al*. [11]. The ANSYS software was used to analyze the hydrodynamic of a TLP with a wind turbine under the impact of waves and wind [12]. Hung *et al*. [13] studied the stability of a tension leg platform using ANSYS software. Gu *et al*. [14] determined the dynamic response of a tension leg platform, and calculated the force exerted on the moorings under random waves with a scale of 1:40, both numerically and experimentally. Pegalajar-Jurado *et al*. [15] studied the hydrodynamics of a TLP with a wind turbine under irregular and concentrated waves in three different numerical methods. Zhao *et al*. [16] investigated the time domain dynamic response analysis of a TLP with a wind turbine under the wave, wind, and combined force. Huang *et al*. [17] studied the dynamic analysis of a tension leg platform with a new wind turbine construction. Ma *et al*. [18] experimentally studied the surge amplitude of a TLP with a wind turbine using the ANSYS AQWA software in the time domain. Tabeshpour *et al*. [19] studied the behavior of a tension leg platform during mooring damage. Madsen *et al*. [20] conducted an experimental dynamic analysis of a TLP with a wind turbine scale of 1:60, using different control techniques. Nematbakhsh *et al*. [21] compared the impacts of wave force on a TLP wind turbine using computational fluid dynamics and potential flow theory methods. Zwickau *et al*. [22] designed a TLP that could be installed in water of 60 m depth and withstand waves of a 50-year return period, wind, and currents. They considered this research in the time domain and under surge, sway, and heave motions, and investigated the force applied to the moorings. Razaghian *et al*. [23] investigated the hydrodynamics of ISSC TLP, and studied the platform's behavior during a tendon cut due to severe sea conditions. At the Marine Engineering Laboratory of Sharif University, Seif *et al*. [24] performed an experimental analysis to obtain a TLP platform's RAO under regular environmental conditions.

In this study, a TLP with the wind turbine is analyzed using two numerical methods; the boundary element method and the finite volume method. First, the platform under regular waves of 1 and 100-year return periods was studied by two numerical methods, and the results obtained were validated. The platform was then analyzed under irregular waves, and finally, the RAO for surge, heave, and pitch motions was computed.

2. Governing equations

2.1. Three-dimensional diffraction theory

This section uses diffraction theory to investigate the dynamic response of an offshore wind turbine installed on a TLP under the applied wind, wave, and current forces. Using the structural elements in the definition of the TLP model with wind turbine and applying the boundary element mesh, different terms of damping, added mass, and force are calculated. In diffraction theory, wave force is calculated by integrating the pressure on the wetted surface of the body. This method can be used when the dimensions of the body are large enough compared to the wave amplitude and wavelength. In the diffraction theory, the flow potential function expresses the fluid flow field. As a result, the potential function should satisfy Laplace's equation. Equation (1) uses the concept of potential superposition principles; the total potential may be calculated as the sum of three terms, incident wave potential, diffracted wave potential, and radiated wave potential. The total Froude-Krylov potential is calculated by adding the potential of the waves and the potential due to wave diffraction [25]:

$$\emptyset_{\mathbf{t}} = \emptyset_{\mathbf{I}} + \emptyset_{\mathbf{D}} + \sum_{\mathbf{R=1}}^{\mathbf{6}} \emptyset_{\mathbf{R}} \quad (1)$$

where $\emptyset_I$ is the incident wave potential, $\emptyset_D$ is the diffraction wave potential, and $\emptyset_R$ is the radiated

potential representing the waves generated due to 6 DOF motions in still water. For a permanently fixed body, $\emptyset_R$ becomes zero. The potential function will be obtained by solving the Laplace equation for incompressible, non-viscous, and non-rotational flow, which is represented as follows:

$$\frac{\partial^2\emptyset}{\partial X^2}+\frac{\partial^2\emptyset}{\partial Y^2}+\frac{\partial^2\emptyset}{\partial Z^2}=0 \quad (2)$$

By assuming the origin of the coordinate system on the water surface, the bottom boundary condition is defined as follows:

$$\frac{\partial\emptyset}{\partial z}=0 \ \text{in} \ z=-h \quad (3)$$

where h is the water depth. The free surface and kinematic boundary conditions are given by (4) and (5), respectively:

$$g\frac{\partial\emptyset}{\partial z}-\omega^2\emptyset=0 \quad (4)$$

$$\frac{\partial\emptyset}{\partial n}=\vec{V}.\vec{n} \quad (5)$$

where ω, $\vec{n}$, and $\vec{V}$ are wave encounter frequency, surface normal vector, and velocity vector of the body, respectively. The far field boundary condition is expressed as follows:

$$|\nabla_\emptyset| \to 0 \ \text{when} \ z \to -\infty \quad (6)$$

By using Green's second identity, the general solution of Laplace equation is as follows:

$$\varepsilon_{(P)}\emptyset=-\int\left(v\frac{\partial\emptyset}{\partial n}-\emptyset\frac{\partial v}{\partial n}\right)ds \quad (7)$$

$\varepsilon_{(P)}$ is equal to 1 when the point P is inside the domain, 0.5 on the boundary, and zero at other points. The wave load, added mass, and damping are also determined from (8) and (9):

$$\vec{F_j}=i\omega p\iint\emptyset\vec{n_j}ds \quad (8)$$

$$R(\omega)+i\omega m_r(\omega)=-i\omega p\iint\emptyset_j\frac{\partial\emptyset_j}{\partial n}ds \quad (9)$$

$\vec{F_j}$ is the wave force vector of the element j, $R(\omega)$ is the damping value, and $m_r(\omega)$ is the added mass. The fluid pressure on the structure is the sum of two components; hydrostatic pressure and hydrodynamic pressure. Hydrodynamic forces are generated by time variation of the potential function. Therefore, the total pressure can be calculated using the following equation:

$$\frac{p}{\rho}=-gz-\frac{\partial\emptyset}{\partial t} \quad (10)$$

The hydrodynamic pressure can be calculated with reference to (11):

$$p_h=-i\rho\omega\emptyset \quad (11)$$

In this method, all hydrodynamic coefficients including added mass, damping matrix, and other hydrodynamic properties are calculated and stored. Finally, considering all of the wave forces and 6-DOF motions, the time history of the motions can be obtained.

2.2. Finite volume method analysis

The finite volume method is a numerical approach for solving partial differential equations like the Navier-Stokes equations. The RANS equations can be used in hydrodynamic modeling of different phenomena such as the analysis of offshore platform, and the study of ship motions and resistance. This approach can use different mathematical models to predict the effects of turbulence. The governing equations for numerical analysis of TLP in waves are Reynolds-averaged Navier–Stokes (RANS) equation, which can be written as follows [26]:

$$\frac{\partial}{\partial x_j}(u_j)=0 \quad (12)$$

$$\frac{\partial}{\partial t}(u_i)+\frac{\partial}{\partial x_j}(u_j u_i)=-\frac{1}{\rho}\frac{\partial p}{\partial x_i}+\frac{1}{\rho}\frac{\partial}{\partial x_j}\left[\mu_{eff}\left(\frac{\partial u_j}{\partial x_i}+\frac{\partial u_i}{\partial x_j}\right)\right]-D_i u_i+g_i \quad (13)$$

In the present work, renormalization group (RNG) k-ε two-equation model is adopted to estimate the turbulence.

3. Dimension of TLP with wind turbine

Figure 2 shows the platform with wind turbine used for BEM numerical analysis. Also the FVM model of TLP with wind turbine is shown in Figure 3. Mesh details of BEM and FVM applied to TLP are shown in Figure 4.

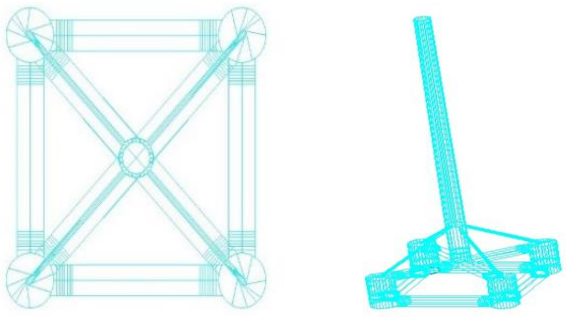

(a) (b)

Figure 2. BEM Model of TLP (a) Top view (b) 3D view

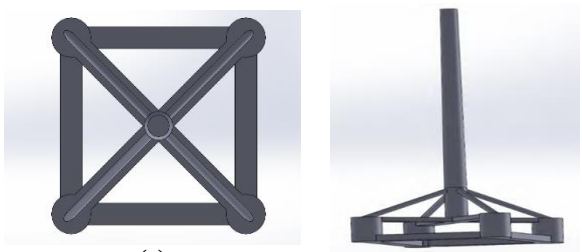

(a) (b)

Figure 3. FVM Model of TLP (a) Top view (b) 3D view.

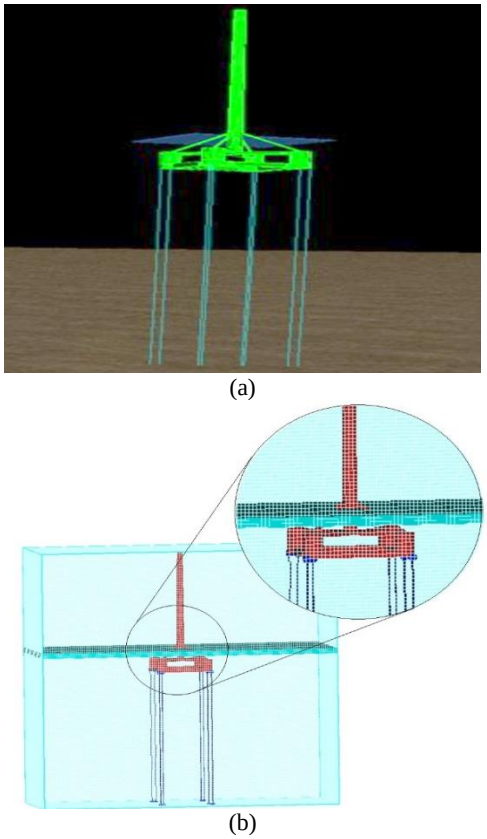

(a) (b)

Figure 4. Mesh details of TLP (a) BEM (b) FVM.

The parameters of TLP and tendon are presented in tables 1 and 2. The research work is carried out according to wave, current, and wind characteristics in the Caspian sea, as given in table 3.

Table 1. Particulars of TLP with wind turbine.

Particulars	Value
Overall length and breadth	49 m
Distance between pantones	40 m
Vertical pantone height	12 m
Vertical pantone diameter	9 m
Horizontal pantone breadth	5 m
Horizontal pantone height	3 m
Pillar diameter	6.5 m
Diagonal leg diameter	1 m
Water depth	150 m
Draft	20 m
Platform pillar height	15 m
Platform weight	2734.2 tones
Turbine leg weight	347.4 tones

The natural period of the platform for 6 degrees of freedom for the depth of 150 m is given in table 4.

Table 2. Particulars of TLP's tendon.

Number of tendons	8
Diameter (mm)	296
Tendon length(m)	130
Breaking load (kN)	24.5×10^3
Axial stiffness of each tendon (kN/m)	5.09×10^3

Table 3. Environmental characteristics of Caspian sea.

Environmental parameter	Return period	
	1-year	100-year
Effective wave height H_S (m)	6.5	9.5
Period T_P (S)	10.3	12.8
Wind velocity (m/s)	21	29
Current velocity (m/s)	0.6	0.9

The safety factors for return period of 1 and 100-year environmental conditions have been investigated using regulations of International Association of Classification Societies (IACS) [27]. The safety factors and the maximum allowable force applied to the moorings are given in table 5.

Table 4. Natural period of TLP for 6 DOF motions.

Motions	Natural period of platform(s)
Surge	30
Sway	30
Heave	1.33
Roll	3.13
Pitch	3.13
Yaw	22.5

Table 5. Safety factor and breaking load for different conditions [27].

Analysis condition	Safety factor	Breaking load (kN)
1-year design	1.1	22.296×10^3
100-year-design	1.8	13.625×10^3

4. Numerical results of BEM and FVM

4.1. Validation of results

In order to validate the BEM and FVM approaches, results were compared for 1 and 100-year regular wave conditions. These results include the time history of the surge motion of TLP and the force applied on moorings No. 1.

4.1.1. Validation for 1-year regular wave

In figures 4, the time history of the surge motion for TLP obtained from BEM and FVM are compared, respectively. The solution time of BEM is much less than FVM. Therefore, for BEM analysis, the solution continued for 800 s but for FVM analysis of TLP, due to the longer solution

time, the solution was performed just for 180 s, and during this time, at least 15 waves encountered the TLP. Figure 4 show that the platform has reached steady conditions in both BEM and FVM approaches after starting seconds in which a significant fluctuation occurs. As it can be seen, the amplitude of the surge motion in BEM numerical method is in good agreement with FVM.

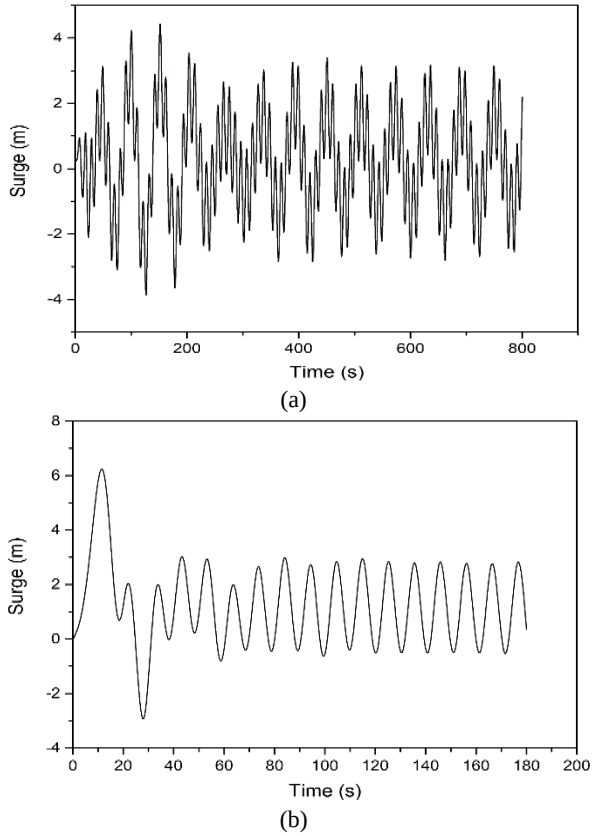

Figure 5. Time history of platform surge motion in 1-year regular wave using (a) BEM (b) FVM.

The time history of the tension force in mooring line No. 1 for 1-year regular wave is shown in figure 5. The results show that there is no significant distinction between the tension in the mooring No. 1 in BEM and FVM approaches. In the BEM results, the minimum and maximum tension in mooring No. 1 are 4.30×10^3 and 5.76×10^3 kN, respectively. In other hand, these values for FVM method are 4.40×10^3 and 5.53×10^3 kN. The results indicate that the maximum tension on the mooring using the BEM numerical analysis is somewhat greater than FVM results; the maximum difference between two numerical methods is 0.23×10^3 kN. According to the above results, it can be stated that the results of the BEM and FVM approaches are acceptable and valid for 1-year regular wave conditions.

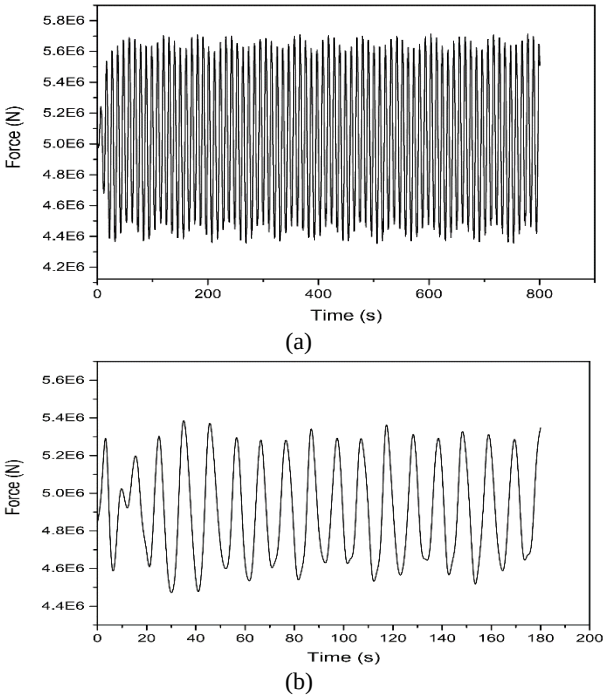

Figure 6. Time history of tension force on the mooring No. 1 for 1-year regular wave using (a) BEM (b) FVM.

4.1.2. Validation for 100-years regular wave

Since 1 and 100-year wave conditions differ in period and wave height, motions and forces of the 100-year wave may damage the platform. Accordingly, validation analysis of two numerical methods was also performed for 100-year return period conditions. In figure 6, the time history of surge motion of TLP in 100-year waves were computed by two numerical methods and compared, respectively.

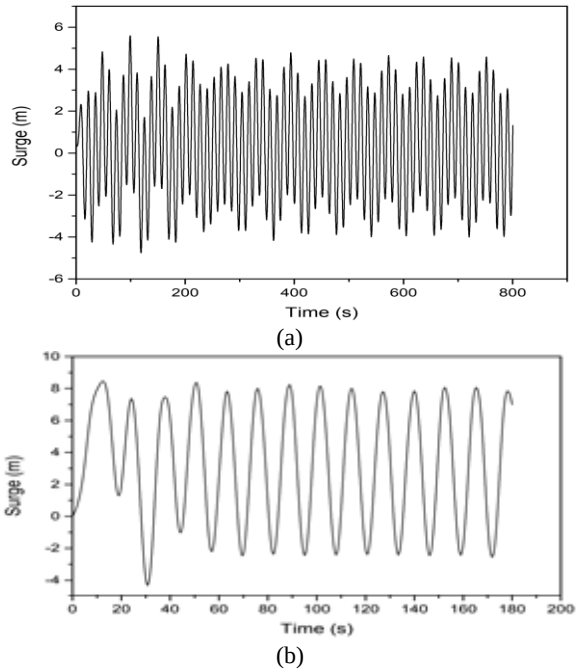

Figure 7. Time history of platform surge motion in 100-year regular wave using (a) BEM (b) FVM.

As evident from figure 6, for the wave of 100-year return period, the results of the two approaches have little difference. Besides, validation was done for the tension force in mooring No. 1 of TLP in 100-year wave conditions; the results are shown in figure 7.

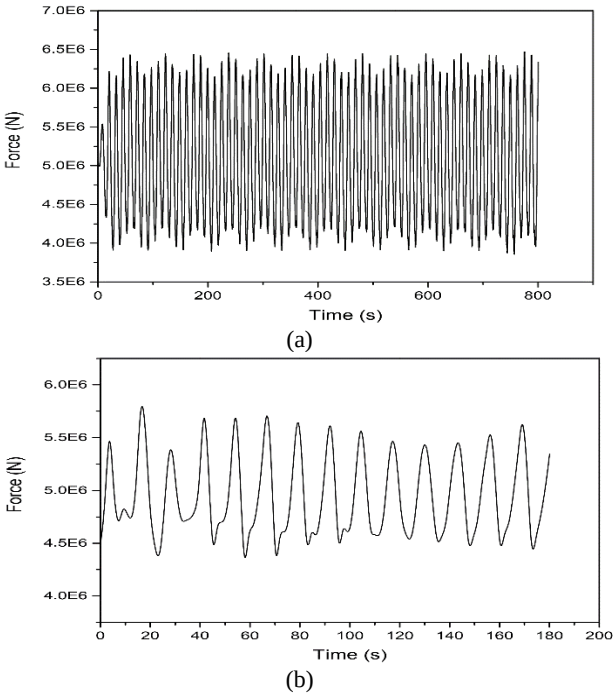

Figure 8. Time history of the force on the mooring No. 1 in 100-year regular wave using (a) BEM (b) FVM.

As it can be seen in figure 7, the tension force calculated by the two methods is very close, and there is not much difference between them. Also the comparison of the tension force in moorings No. 1 and 3 show that these mooring lines have similar behavior because moorings No. 1 is on the left side, whereas moorings No. 3 is on the right side of the TLP (Figure 1). The difference in maximum tension of the moorings No. 1 and 3 is 0.64×10^3 and 0.46×10^3 kN, respectively. These results show that these methods are valid for study of TLP in different wave conditions.

4.2. Comparison of tensions regarding to IACS regulations

For the safe design of platforms, it is necessary to compare the tension forces with the regulations to determine the ability of mooring lines to withstand the tensions. In this study, using the IACS Code, the maximum allowable tension in moorings was calculated considering the safety factors and given in table 5. From the results in figures 5 and 7, it can be seen that for 1-year regular wave condition, the maximum tension in the mooring lines according to BEM and FVM numerical analysis is 5.76×10^3 and 5.59×10^3 kN, respectively. Besides, for the wave of 100-year return period, it increases to 6.59×10^3 and 6.10×10^3 kN, respectively. Comparing the above results with the values of 22.295×10^3 kN in 1-year and 13.625×10^3 kN for 100-year, it can be concluded that the tensions applied to the moorings are within the maximum permissible tension range.

5. TLP Analysis in Irregular Wave

After validating the two methods, the main study of the TLP can be performed; the analysis of TLP in irregular waves of 1 and 100-year return period, and then analyzing the RAO of the platform.

5.1. TLP analysis in 1-year irregular wave

For study of TLP in irregular waves, the modified JONSWAP spectrum was selected for the wave load, whose the spectral function is as follows [28]:

$$\boldsymbol{S(f) = \beta_j H_{\frac{1}{3}}^2 f^{-5} T_P^{-4} \exp[-1.25\,(T_P f)^{-4}]} \quad (18)$$
$$\times \boldsymbol{\gamma^{exp[-(T_P f-1)^2/2\delta^2]}}$$

where f, T_P, and $H_{1/3}$ are wave frequency, peak period, and significant wave height, respectively. Other parameters are defined as follows:

$$\gamma = \begin{cases} 5 & T_P/\sqrt{H_{1/3}} \le 3.6 \\ exp[5.75 - 1.15\,T_P/\sqrt{H_{1/3}}] & 3.6 < T_P/\sqrt{H_{1/3}} < 5 \\ 1 & T_P/\sqrt{H_{1/3}} \ge 5 \end{cases}$$

$$\delta = \begin{cases} 0.07 & f \le f_P \\ 0.09 & f \ge f_P \end{cases} \quad (19)$$

$$\beta_j = \frac{0.06238[1.094 - 0.01915\,ln\,\gamma]}{0.23 + 0.0336\gamma - 0.185(1.9+\gamma)^{-1}}$$

$$T_P = \frac{T_{1/3}}{[1 - 0.132(\gamma + 0.2)]^{-0.559}}$$

The time history of surge motion of TLP in 1-year irregular waves calculated by BEM and FVM methods are shown in figure 8. According to the data in figure 8, it can be seen that the surge motion calculated by the BEM method agree well with FVM results. The maximum surge in 1-year irregular wave conditions by BEM and FVM analysis is 4.02 and 5.02 m, respectively.

A comparison of the tension force in mooring No. 1, calculated by two approaches, is presented in figure 9. From figure 9, it can be seen that the tension of BEM is consistent with the FVM results. The maximum tension in mooring No. 1 obtained by BEM and FVM methods is 5.79×10^3 and 5.59×10^3 kN, respectively. It should be noted that these tension forces are within the permissible limits according to ICAS regulations. The results indicate that both numerical approaches can be

used to study floating platforms in irregular waves.

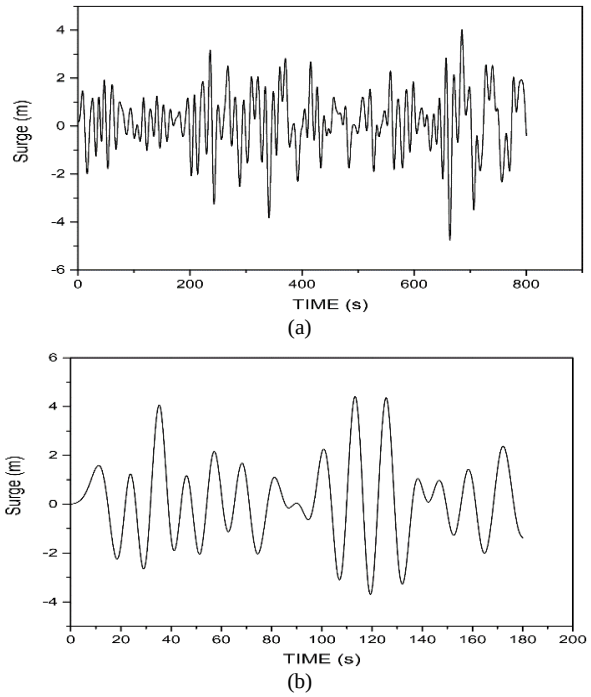

Figure 9. Time history of platform surge motion in 1-year irregular wave using (a) BEM (b) FVM.

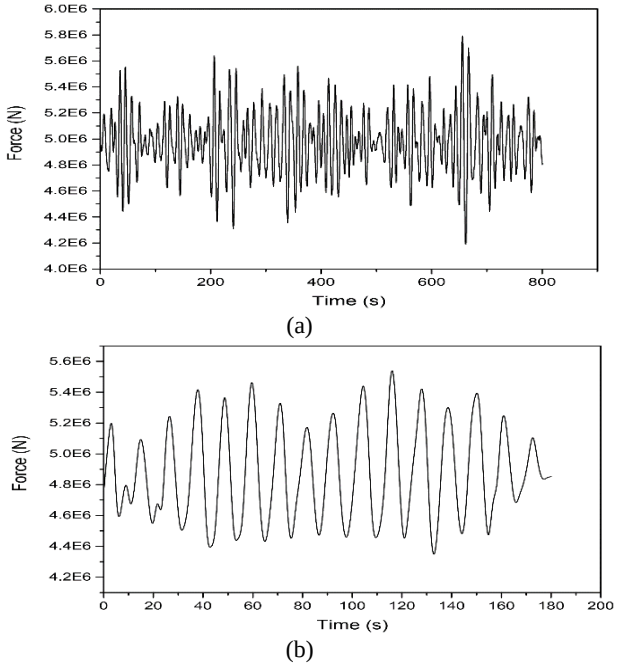

Figure 10. Time history of the force on the mooring No. 1 in 1-year irregular wave using (a) BEM (b) FVM.

5.2. TLP analysis in 100-year irregular wave

As a prediction of the most extreme wave that can be expected to occur, the 100-year wave commonly taken into consideration by designers of oil platforms and other offshore structures [29]. In this section, the effect of 100-year irregular wave conditions is studied on the motions and mooring tensions of the TLP. Time history of surge and motion of TLP under 100-year irregular wave is shown in figure 10.

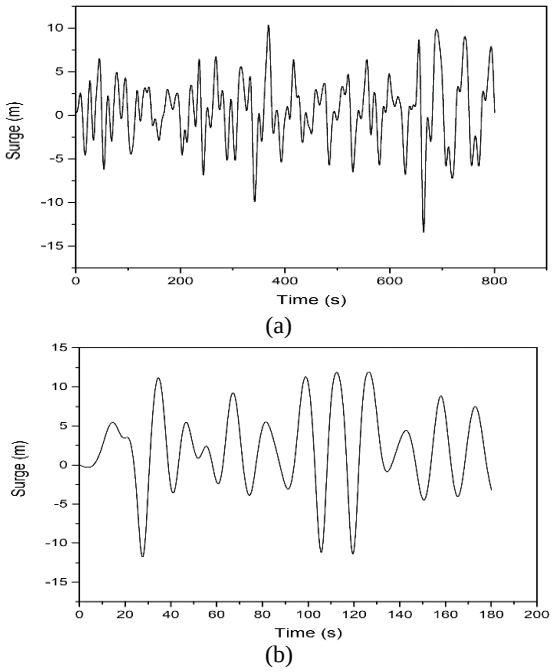

Figure 11. Time history of platform surge motion in 100-year irregular wave using (a) BEM (b) FVM.

As it can be seen in figure 10, in 100-year irregular wave, the maximum surge of TLP calculated by BEM and FVM is 10.31 and 12.19 m, respectively. It can be stated that the surge motion computed by the BEM have good agreement with the FVM results. The time history of tension force in mooring No. 1 of TLP is depicted in figure 11.

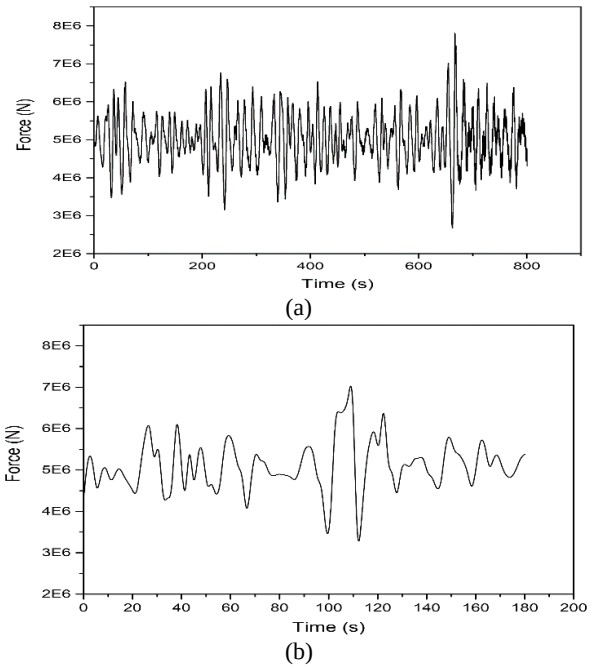

Figure 12. Time history of the force on the mooring No. 1 in 100-year irregular wave using (a) BEM (b) FVM.

According to figure 11, it is evident that the tension forces in the mooring lines No. 1 obtained by BEM agree well with the FVM results. The difference in the maximum tension between two numerical methods for mooring No. 1 is 0.37 × 10^3 kN.

5.3. RAO analysis of TLP with wind turbine

Response amplitude operator (RAO) of TLP motions is obtained using the BEM and FVM approaches. For this, an irregular 100-year wave encountered the TLP in a water depth of 150 m, and the platform's surge, heave, and pitch motions were calculated. Figure 12 shows these RAO diagrams for two numerical methods.

As previously seen, TLP motions and mooring tensions in the two numerical methods have a good agreement under both regular and irregular waves. In figure 12, it is evident that RAO diagrams in the three motions also are in good agreement for the BEM and FVM approaches. According to figure 12-a, which depicts the RAO for surge motion, in both numerical methods, by increase in the wave period, which means the increase in wavelength, the forces acting on TLP increased, which raised the surge motion. As seen in figure 12-b, the rise of the wave period from 7 to 11 s causes the heave motion to increase to a peak and drop between 11 and 18 s. After a wave period of 18 s, heave motion grows gradually. Moreover, figure 12-c shows that the pitch motion rises sharply by increasing the wave period from 6.5 to 9 s, then reducing gently.

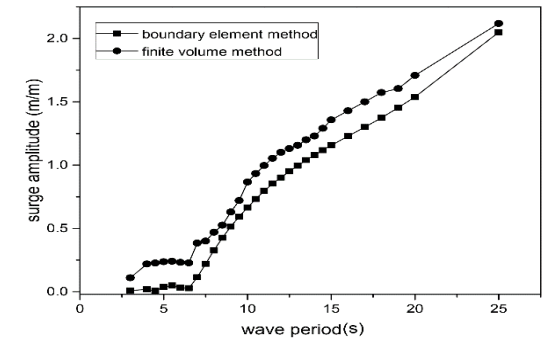

(a)

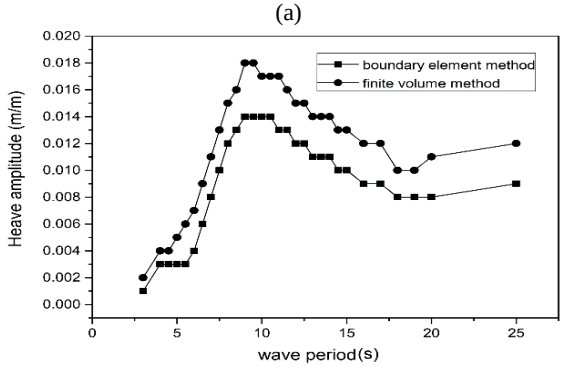

(b)

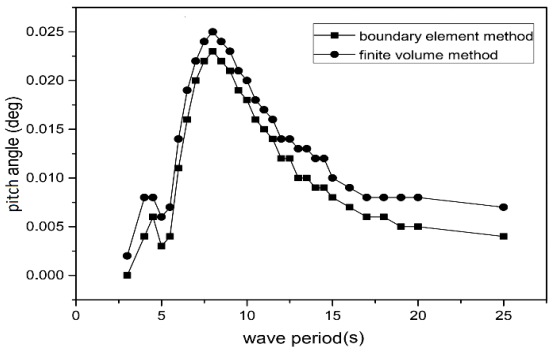

(c)

Figure 13. RAO diagrams for motions of TLP with a wind turbine (a) surge (b) heave (c) pitch.

6. Conclusion

The primary purpose of this study was to investigate a wind turbine installed on an offshore platform under 1 and 100-years regular and irregular waves in the Caspian sea. This research work utilized numerical analysis by the boundary element method and the finite volume method to investigate the surge and heave motions and the tension force in the mooring lines. In this work, according to more solution time, the FVM analysis of TLP was done for 180 s but the BEM solution was carried out for 800 s. However, the data shows that all the surge, heave, mooring tensions, and RAO values agree well in both numerical methods. One of the main reasons for differences in the results is neglecting the viscosity in the boundary element method. In general, it can be concluded that the performance of these two approaches has been acceptable.

6. References

[1] Abazari, A., Dynamic Response of a Combined Spar-Type FOWT and OWC-WEC by a Simplified Approach. Renewable Energy Research and Applications, 2023. 4(1): p. 66-77.

[2] Han, Y. et al., Stability and dynamic response analysis of a submerged tension leg platform for offshore wind turbines. Ocean engineering, 2017. 129: p. 68-82.

[3] Oguz, E. et al., Experimental and numerical analysis of a TLP floating offshore wind turbine. Ocean Engineering, 2018. 147: p. 591-605.

[4] Abdussamie, N. et al., Experimental investigation of wave-in-deck impact events on a TLP model. Ocean Engineering, 2017. 142: p. 541-562.

[5] Abrishamchi, A. and B. Younis, LES and URANS predictions of the hydrodynamic loads on a tension-leg platform. Journal of fluids and structures, 2012. 28: p. 244-262.

[6] Kim, C.-H., C.-H. Lee, and J.-S. Goo, A dynamic response analysis of tension leg platforms including

hydrodynamic interaction in regular waves. Ocean engineering, 2007. 34(11-12): p. 1680-1689.

[7] Bachynski, E.E. and T. Moan, Design considerations for tension leg platform wind turbines. Marine Structures, 2012. 29(1): p. 89-114.

[8] Senjanović, I., M. Tomić, and S. Rudan, Investigation of nonlinear restoring stiffness in dynamic analysis of tension leg platforms. Engineering structures, 2013. 56: p. 117-125.

[9] Yu, Y. et al., Investigation of TLP's hydrodynamic response with different tendon connection angles. Theoretical and Applied Mechanics Letters, 2018. 8(4): p. 291-297.

[10] Gu, J.-y., J.-m. Yang, and H.-n. Lv, Studies of TLP dynamic response under wind, waves and current. China Ocean Engineering, 2012. 26(3): p. 363-378.

[11] Ren, N. et al., Experimental and numerical study of dynamic responses of a new combined TLP type floating wind turbine and a wave energy converter under operational conditions. Renewable Energy, 2020. 151: p. 966-974.

[12] Chodnekar, Y.P. and S. Mandal, Hydrodynamic analysis of floating offshore wind turbine. Procedia Engineering, 2015. 116: p. 4-11.

[13] Huang, R. et al. Study on Mooring Economy and Stability of Floating Wind Turbine. in 2020 5th Asia Conference on Power and Electrical Engineering (ACPEE). 2020. IEEE.

[14] Gu, J.-y., J.-m. Yang, and H.-n. Lü, Numerical simulations and model tests of the mooring characteristic of a tension leg platform under random waves. China Ocean Engineering, 2013. 27(5): p. 563-578.

[15] Pegalajar-Jurado, A., H. Bredmose, and M. Borg, Multi-level hydrodynamic modelling of a scaled 10MW TLP wind turbine. Energy Procedia, 2016. 94: p. 124-132.

[16] Zhao, Y.-s. et al., Coupled dynamic response analysis of a multi-column tension-leg-type floating wind turbine. China Ocean Engineering, 2016. 30(4): p. 505-520.

[17] Huang, H. and S.-r. Zhang, Dynamic analysis of tension leg platform for offshore wind turbine support as fluid-structure interaction. China Ocean Engineering, 2011. 25(1): p. 123-131.

[18] Ma, Z. et al., Experimental and numerical study on the multi-body coupling dynamic response of a Novel Serbuoys-TLP wind turbine. Ocean Engineering, 2019. 192: p. 106570.

[19] Tabeshpour, M.R., A. Ahmadi, and E. Malayjerdi, Investigation of TLP behavior under tendon damage. Ocean Engineering, 2018. 156: p. 580-595.

[20] Madsen, F. et al., Experimental analysis of the scaled DTU10MW TLP floating wind turbine with different control strategies. Renewable Energy, 2020. 155: p. 330-346.

[21] Nematbakhsh, A. et al., Comparison of wave load effects on a TLP wind turbine by using computational fluid dynamics and potential flow theory approaches. Applied Ocean Research, 2015. 53: p. 142-154.

[22] Żywicki, J. et al., Design of structure of Tension Leg Platform for 6 MW offshore wind turbine based on FEM analysis. Polish Maritime Research, 2017.

[23] Razaghian, A., M. Seif, and M. Tabeshpour, Investigation of tendons and TLP behavior in damaged condition. Journal Of Marine Engineering, 2014. 9(18): p. 23-34.

[24] Seif, M., A. Razaghian, and M. Tabeshpour, EXPERIMENTAL MODELING REQUIREMENTS FOR TLP PLATFORMS. 2013.

[25] Journee, J.M. and W. Massie, Introduction in offshore hydromechanics (OT3600). TUDelft, Faculty of Marine Technology, Ship Hydromechanics Laboratory, Report No. 1267-K, Lecture Notes, 2001.

[26] Yakhot, V. et al., Development of turbulence models for shear flows by a double expansion technique. Physics of Fluids A: Fluid Dynamics, 1992. 4(7): p. 1510-1520.

[27] Nersesian, R. and S. Mahmood, International association of classification societies, in Handbook of Transnational Economic Governance Regimes. 2010, Brill Nijhoff. p. 765-774.

[28] Goda, Y., Statistical variability of sea state parameters as a function of wave spectrum. Coastal Engineering in Japan, 1988. 31(1): p. 39-52.

[29] Goda, Y., Random seas and design of maritime structures. Vol. 33. 2010: World Scientific Publishing Company.